



Fritsch, D., & Annett, J. F. (2015). Triplet superconductivity and proximity effect induced by Bloch and Néel domain walls. *Superconductor Science and Technology*, 28(8), [085015]. DOI: 10.1088/0953-2048/28/8/085015

Publisher's PDF, also known as Version of record

License (if available):
CC BY

Link to published version (if available):
[10.1088/0953-2048/28/8/085015](https://doi.org/10.1088/0953-2048/28/8/085015)

[Link to publication record in Explore Bristol Research](#)
PDF-document

This is the final published version of the article (version of record). It first appeared online via IOP Publishing at <http://iopscience.iop.org/article/10.1088/0953-2048/28/8/085015>. Please refer to any applicable terms of use of the publisher.

University of Bristol - Explore Bristol Research

General rights

This document is made available in accordance with publisher policies. Please cite only the published version using the reference above. Full terms of use are available:
<http://www.bristol.ac.uk/pure/about/ebr-terms.html>

Triplet superconductivity and proximity effect induced by Bloch and Néel domain walls

This content has been downloaded from IOPscience. Please scroll down to see the full text.

2015 Supercond. Sci. Technol. 28 085015

(<http://iopscience.iop.org/0953-2048/28/8/085015>)

View [the table of contents for this issue](#), or go to the [journal homepage](#) for more

Download details:

IP Address: 137.222.10.113

This content was downloaded on 11/02/2016 at 10:00

Please note that [terms and conditions apply](#).

Triplet superconductivity and proximity effect induced by Bloch and Néel domain walls

Daniel Fritsch* and James F Annett

H. H. Wills Physics Laboratory, School of Physics, University of Bristol, Bristol BS8 1TL, UK

E-mail: d.fritsch@bath.ac.uk

Received 25 March 2015, revised 20 May 2015

Accepted for publication 27 May 2015

Published 13 July 2015



CrossMark

Abstract

Noncollinear magnetic interfaces introduced in superconductor (SC)/ferromagnet/SC heterostructures allow for spin-flipping processes and are able to generate equal-spin spin-triplet pairing correlations within the ferromagnetic region. This leads to the occurrence of the so-called long-range proximity effect. Particular examples of noncollinear magnetic interfaces include Bloch and Néel domain walls. Here, we present results for heterostructures containing Bloch and Néel domain walls based on self-consistent solutions of the spin-dependent Bogoliubov–de Gennes equations in the clean limit. In particular, we investigate the thickness dependence of Bloch and Néel domain walls on induced spin-triplet pairing correlations and compare with other experimental and theoretical results, including conical magnetic layers as noncollinear magnetic interfaces. It is shown that both Bloch and Néel domain walls lead to the generation of unequal-spin spin-triplet pairing correlations of similar strength as for conical magnetic layers. However, for the particular heterostructure geometries investigated, only Bloch domain walls lead to the generation of equal-spin spin-triplet pairing correlations. They are stronger than those generated by an equivalent thickness of conical magnetic layers. In order for Néel domain walls to induce equal-spin spin-triplet pairing correlations, they have to be oriented such that the noncollinearity appears within the plane parallel to the interface region.

Keywords: proximity effect, multilayers, heterostructures, nonconventional superconductivity

(Some figures may appear in colour only in the online journal)

1. Introduction

Bringing a superconductor (SC) and a ferromagnetic (FM) material in close proximity to each other results in drastic changes for the spin-singlet Cooper pairs. While the Pauli principle requires the spins to orient parallel in the FM region, the spin-singlet Cooper pair electrons tend to align antiparallel in the SC region. This leads to the following consequences: (i) different Fermi velocities in the spin-up and spin-down channel of the electrons due to the exchange field lead to a centre of mass modulation and an oscillating behaviour of the superconducting correlations within the FM region [1–3],

namely the FFLO oscillations [4, 5]. Unequal-spin spin-triplet correlations ($S_z = 0$) are also generated. Both of these correlations are oscillating and suppressed in the FM region, and are essentially short-range. (ii) Following a theoretical suggestion by Bergeret *et al* [6] it should also be possible to induce equal-spin spin-triplet Cooper pairs which are compatible with and unaffected by the FM exchange field, thus leading to much larger penetration depths. This phenomenon requires spin-flip processes at the interface and is called the long-range proximity effect.

Since this first theoretical prediction equal-spin spin-triplet pairing correlations have attracted a lot of attention and are reviewed by Buzdin [7], Bergeret *et al* [8], and Tanaka *et al* [9]. Several multilayer setups have been suggested experimentally and theoretically to shed some light on the

* Present address: Department of Chemistry, University of Bath, Claverton Down, Bath, BAZ 7AY, UK.



specific interface properties necessary to generate equal-spin spin-triplet pairing correlations within such structures. These setups typically involve noncollinear magnetic structures within the interface region as provided by different FM layers [10, 11], helical (or conical) magnetic layers [12–16], or through specific interface potentials [17–20]. Moreover, also the effects of Bloch [14, 15, 21] and Néel [14, 15, 21, 22] domain walls, as well as interfacial spin–orbit coupling [23, 24] as source for generating equal-spin spin-triplet pairing correlations have been investigated.

On the theoretical side, equal-spin spin-triplet pairing correlations have been investigated using Green’s function techniques based on solutions of the Usadel equations [12, 14, 15, 21], and self-consistent solutions of the Bogoliubov–de Gennes (BdG) equations [16, 17]. While the Green’s function techniques allow for an easier inclusion of scattering effects describing a shorter electron mean free path in the diffusive limit, these effects can in principle be incorporated into the BdG equations as well via additional impurity scattering potentials. However, in the present work we are solely concerned with the special case of odd-frequency triplet pairing correlations, which are not affected by non-magnetic impurities [8]. The inclusion of additional impurity scattering potentials would require further investigations.

The main aim of the paper is to assess the effectiveness of Bloch and Néel domain walls in comparison to conical magnetic layers to generate long-range proximity effects. This is motivated by the potential use of magnetic domain walls incorporated in experimental heterostructures to allow for a switching of the generated long-range spin-triplet Josephson current. Based on an established heterostructure setup successfully used in previous experimental and theoretical works we introduce Bloch and Néel domain walls in the interface regions and investigate its suitability to generate equal-spin spin-triplet pairing correlations. These results will be compared to the corresponding results with interface regions containing conical magnetic layers of varying thicknesses.

This paper is organised as follow. Section 2 gives an overview over the theoretical methods. This includes a description of the microscopic BdG equations in section 2.1, and the definition of the spin-triplet pairing correlations in section 2.2. The results for heterostructures containing Bloch and Néel domain walls of varying thicknesses n_{Bloch} and $n_{\text{Néel}}$ are presented in sections 3.1 and 3.2, respectively. Section 4 provides a summary and an outlook.

2. Theoretical background

2.1. BdG equations and heterostructure setup

The results presented in this paper are obtained by means of the microscopic BdG equations, which have been solved self-consistently in the clean limit. In the most general spin-dependent case and incorporating an expression for arbitrary exchange fields \mathbf{h} needed later to describe the influence of

Bloch and Néel domain walls, the BdG equations read [16, 25, 26]

$$\begin{pmatrix} \mathcal{H}_0 - h_z & -h_x + ih_y & \Delta_{\uparrow\uparrow} & \Delta_{\uparrow\downarrow} \\ -h_x - ih_y & \mathcal{H}_0 + h_z & \Delta_{\downarrow\uparrow} & \Delta_{\downarrow\downarrow} \\ \Delta_{\uparrow\uparrow}^* & \Delta_{\downarrow\uparrow}^* & -\mathcal{H}_0 + h_z & h_x + ih_y \\ \Delta_{\uparrow\downarrow}^* & \Delta_{\downarrow\downarrow}^* & h_x - ih_y & -\mathcal{H}_0 - h_z \end{pmatrix} \begin{pmatrix} u_{n\uparrow} \\ u_{n\downarrow} \\ v_{n\uparrow} \\ v_{n\downarrow} \end{pmatrix} = \varepsilon_n \begin{pmatrix} u_{n\uparrow} \\ u_{n\downarrow} \\ v_{n\uparrow} \\ v_{n\downarrow} \end{pmatrix}, \quad (1)$$

where ε_n , $u_{n\sigma}$, and $v_{n\sigma}$ denote eigenvalues, and quasiparticle and quasihole amplitudes for spin σ , respectively. Following simplifications introduced earlier [16, 27, 28] the tight-binding Hamiltonian \mathcal{H}_0 in (1) becomes effectively one-dimensional and reads

$$\mathcal{H}_0 = -t \sum_n (c_n^\dagger c_{n+1} + c_{n+1}^\dagger c_n) + \sum_n (\varepsilon_n - \mu) c_n^\dagger c_n. \quad (2)$$

Therein, c_n^\dagger and c_n denote electronic creation and destruction operators at multilayer index n , respectively. In order to compare the present results with those obtained previously [16, 29, 30] we choose the next-nearest neighbour hopping parameter $t = 1$ and set the energy scales via the chemical potential (Fermi energy) $\mu = 0$.

Balian and Werthamer [31, 32] introduced a way to rewrite the general form of the pairing matrix appearing in (1) as

$$\begin{pmatrix} \Delta_{\uparrow\uparrow} & \Delta_{\uparrow\downarrow} \\ \Delta_{\downarrow\uparrow} & \Delta_{\downarrow\downarrow} \end{pmatrix} = (\Delta + \hat{\boldsymbol{\sigma}} \cdot \mathbf{d}) i\hat{\sigma}_2 = \begin{pmatrix} -d_x + id_y & \Delta + d_z \\ -\Delta + d_z & d_x + id_y \end{pmatrix}. \quad (3)$$

Here, $\hat{\sigma}_2$ denotes a 2×2 matrix. Making additional use of the Pauli matrices $\hat{\boldsymbol{\sigma}}$, the superconducting order parameter is now written as a singlet (scalar) part Δ and a triplet (vector) part \mathbf{d} , respectively. This work is restricted to s -wave SCs, and the pairing potential entering (1) simplifies to a scalar quantity Δ , which fulfills the self-consistency condition

$$\Delta(\mathbf{r}) = \frac{g(\mathbf{r})}{2} \sum_n (u_{n\uparrow}(\mathbf{r}) v_{n\downarrow}^*(\mathbf{r}) [1 - f(\varepsilon_n)] + u_{n\downarrow}(\mathbf{r}) v_{n\uparrow}^*(\mathbf{r}) f(\varepsilon_n)). \quad (4)$$

The sum is evaluated only over positive eigenvalues ε_n and $f(\varepsilon_n)$ denotes the Fermi distribution function evaluated as a step function for zero temperature.

The heterostructure is set up as generally shown in figure 1(a) with a lattice constant $a = 1$ and a strength of the exchange field $h_0 = 0.1$. The effective superconducting coupling parameter $g(\mathbf{r})$ equals 1 in the $n_{\text{SC}} = 250$ left and right layers of spin-singlet s -wave SC and vanishes elsewhere. Between the s -wave SCs and $n_{\text{FM}} = 100$ layers of the FM middle layer we introduce conical magnetic layers (figure 1(a)), and Bloch (figure 1(c)) and Néel (figure 1(d)) domain walls of varying thicknesses n_{CM} , n_{Bloch} , and $n_{\text{Néel}}$, respectively. The conical magnetic layers are arranged as in our previous works [16, 30] and are chosen to represent the conical magnet Holmium. The maximum number of conical

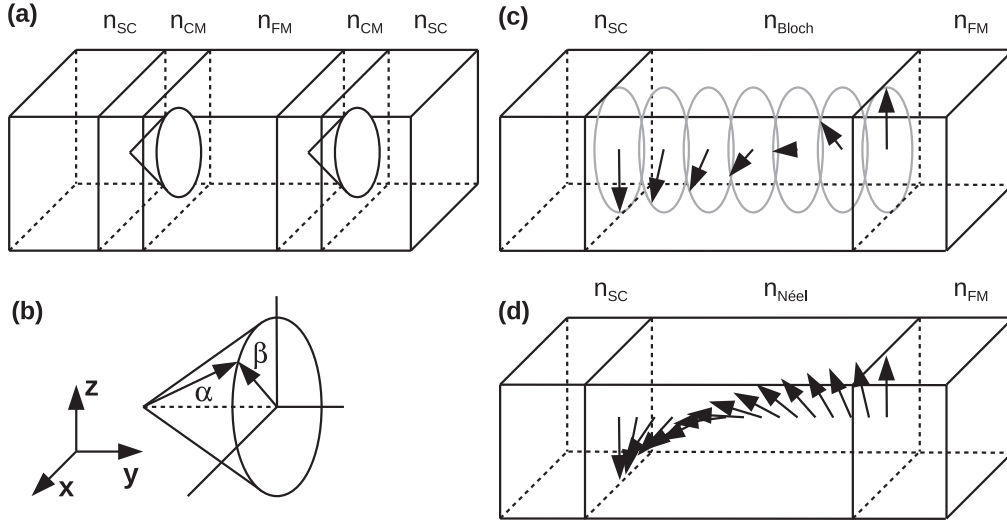


Figure 1. Structural setup of the heterostructures investigated in this work: (a) general setup including n_{SC} layers of s -wave superconductor to the left, n_{CM} layers of a conical magnet, n_{FM} layers of ferromagnetic middle layer, and n_{CM} conical magnet and n_{SC} s -wave superconductor layers to the right. (b) Employed coordinate system and definition of the opening angle α and the turning (or pitch) angle β of the conical magnetic structure. (c) Orientation of the Bloch domain wall of n_{Bloch} layers between the left s -wave superconductor and the middle ferromagnetic region. (d) Orientation of the Néel domain wall of $n_{Néel}$ layers between the left s -wave superconductor and the middle ferromagnetic region. Note that (c) and (d) only show the left interface region for clarity.

magnetic layers considered here correspond to one full turn of the magnetisation around the cone. The Holmium opening angle $\alpha = 80^\circ$ and turning (or pitch) angle $\beta = 30^\circ$ are measured from the positive y axis towards the positive z axis and from the positive z axis towards the positive x axis, respectively (figure 1(b)). The Bloch and Néel domain walls are arranged such that there is a FM coupling to the middle FM region of the heterostructure and that a C_2 symmetry along the central z axis is retained.

2.2. (Triplet) pairing correlations

The specific superconducting pairing correlation between spins α and β we are interested in here is evaluated as on-site interaction for times $t = \tau$ and $t' = 0$ as

$$f_{\alpha\beta}(\mathbf{r}, \tau, 0) = \frac{1}{2} \langle \hat{\Psi}_\alpha(\mathbf{r}, \tau) \hat{\Psi}_\beta(\mathbf{r}, 0) \rangle. \quad (5)$$

Therein, $\hat{\Psi}_\sigma(\mathbf{r}, \tau)$ denotes the many-body field operator for spin σ at time τ , and time-dependence is introduced through the Heisenberg equation of motion. The particular pairing correlation of (5) is local in space and leads to vanishing triplet contributions for $\tau = 0$, in accordance with the Pauli principle [33]. However, finite values of τ give rise to nonvanishing pairing correlations, being an example of odd-frequency triplet pairing [8]. Substituting the field operators valid for our setup and phase convention the spin-dependent triplet pairing correlations read [29, 30]

$$\begin{aligned} f_0(y, \tau) &= \frac{1}{2} (f_{\uparrow\downarrow}(y, \tau) + f_{\downarrow\uparrow}(y, \tau)) \\ &= \frac{1}{2} \sum_n (u_{n\uparrow}(y)v_{n\downarrow}^*(y) + u_{n\downarrow}(y)v_{n\uparrow}^*(y)) \zeta_n(\tau), \end{aligned}$$

$$\begin{aligned} f_1(y, \tau) &= \frac{1}{2} (f_{\uparrow\uparrow}(y, \tau) - f_{\downarrow\downarrow}(y, \tau)) \\ &= \frac{1}{2} \sum_n (u_{n\uparrow}(y)v_{n\uparrow}^*(y) - u_{n\downarrow}(y)v_{n\downarrow}^*(y)) \zeta_n(\tau), \end{aligned} \quad (6)$$

depending on position y within the heterostructure and time parameter τ (set to $\tau = 10$ in the present work), and with $\zeta_n(\tau)$ given by

$$\zeta_n(\tau) = \cos(\varepsilon_n \tau) - i \sin(\varepsilon_n \tau) (1 - 2f(\varepsilon_n)). \quad (7)$$

Based on the rewritten form of the pairing matrix in (3) and defining $\hat{\Delta}$ as the triplet pairing matrix for an ordinary spin-triplet superconductor, the product $\hat{\Delta} \hat{\Delta}^\dagger$ can be written as

$$\hat{\Delta} \hat{\Delta}^\dagger = |\mathbf{d}|^2 \hat{\sigma}_0 + i(\mathbf{d} \times \mathbf{d}^*) \hat{\boldsymbol{\sigma}}. \quad (8)$$

Therein, the magnitude of the \mathbf{d} -vector denotes the gap function independently from the underlying coordinate system, and $i\mathbf{d} \times \mathbf{d}^*$ is a measure of the spin magnetic moment, respectively. In the present work there is no pairing interaction considered in the triplet channel, i.e., $g(\mathbf{r}) = 1$ in (4). However, triplet pairing correlations are induced which are given by the so-called triplet pair correlation function matrix instead, which can be written similarly to the pairing matrix $\hat{\Delta}$ as [30, 34]

$$\hat{f} = (\hat{\boldsymbol{\sigma}} \cdot \mathbf{f}) i \hat{\sigma}_2 = \begin{pmatrix} -f_x + if_y & f_z \\ f_z & f_x + if_y \end{pmatrix}. \quad (9)$$

With (9) the analogue to (8) can be written as

$$\hat{f} \hat{f}^\dagger = |\mathbf{f}|^2 \hat{\sigma}_0 + i(\mathbf{f} \times \mathbf{f}^*) \hat{\boldsymbol{\sigma}}. \quad (10)$$

Analogously to $|\mathbf{d}|$ and $\mathbf{d} \times \mathbf{d}^*$ we find $|\mathbf{f}|$ and $\mathbf{f} \times \mathbf{f}^*$. Again, they can be rewritten in terms of the \mathbf{f} -vector components

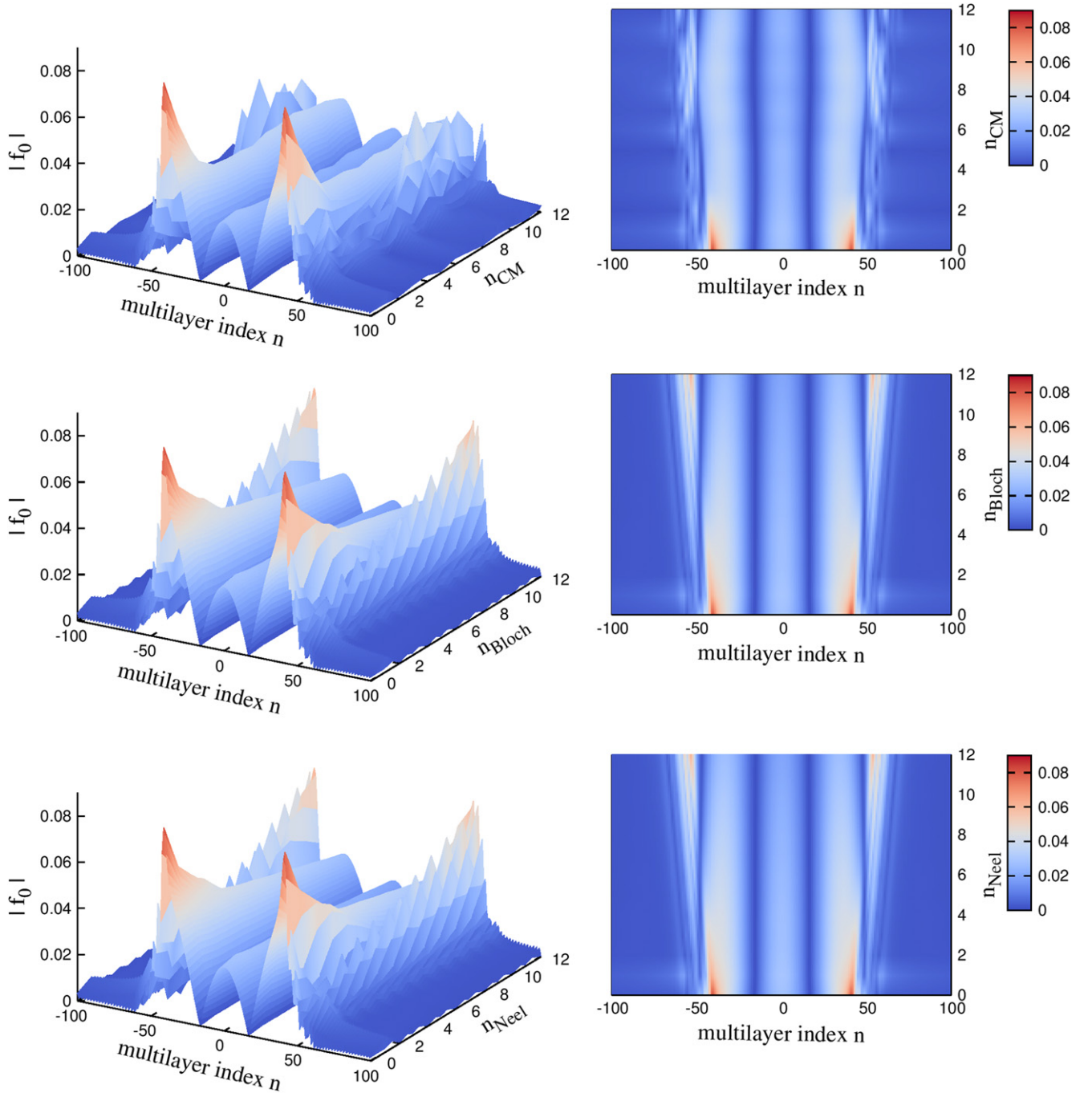


Figure 2. Magnitude of the unequal-spin spin-triplet pairing correlations f_0 for heterostructures containing conical magnetic layers n_{CM} (upper panels), Bloch domain walls n_{Bloch} (middle panels), and Néel domain walls n_{Neel} (lower panels), respectively. The left and right panels both show the full data sets and the right panels show a top view of the data.

which depend on the spin-dependent triplet pairing correlations as

$$\begin{aligned}
 f_x &= \frac{1}{2}(-f_{\uparrow\uparrow} + f_{\downarrow\downarrow}), \\
 f_y &= -\frac{i}{2}(f_{\uparrow\uparrow} + f_{\downarrow\downarrow}), \\
 f_z &= \frac{1}{2}(f_{\uparrow\downarrow} + f_{\downarrow\uparrow}).
 \end{aligned}
 \tag{11}$$

3. Results and discussion

3.1. Heterostructure including Bloch domain walls

The results presented in this section are obtained for heterostructures containing Bloch domain walls of increasing thickness n_{Bloch} to either side of the FM middle layer. The Bloch domain walls are oriented such that the magnetic moments at the interface align parallel to the FM middle layers (figure 1(c)) and that a C_2 symmetry along the central z axis is retained. Recently, heterostructures containing conical

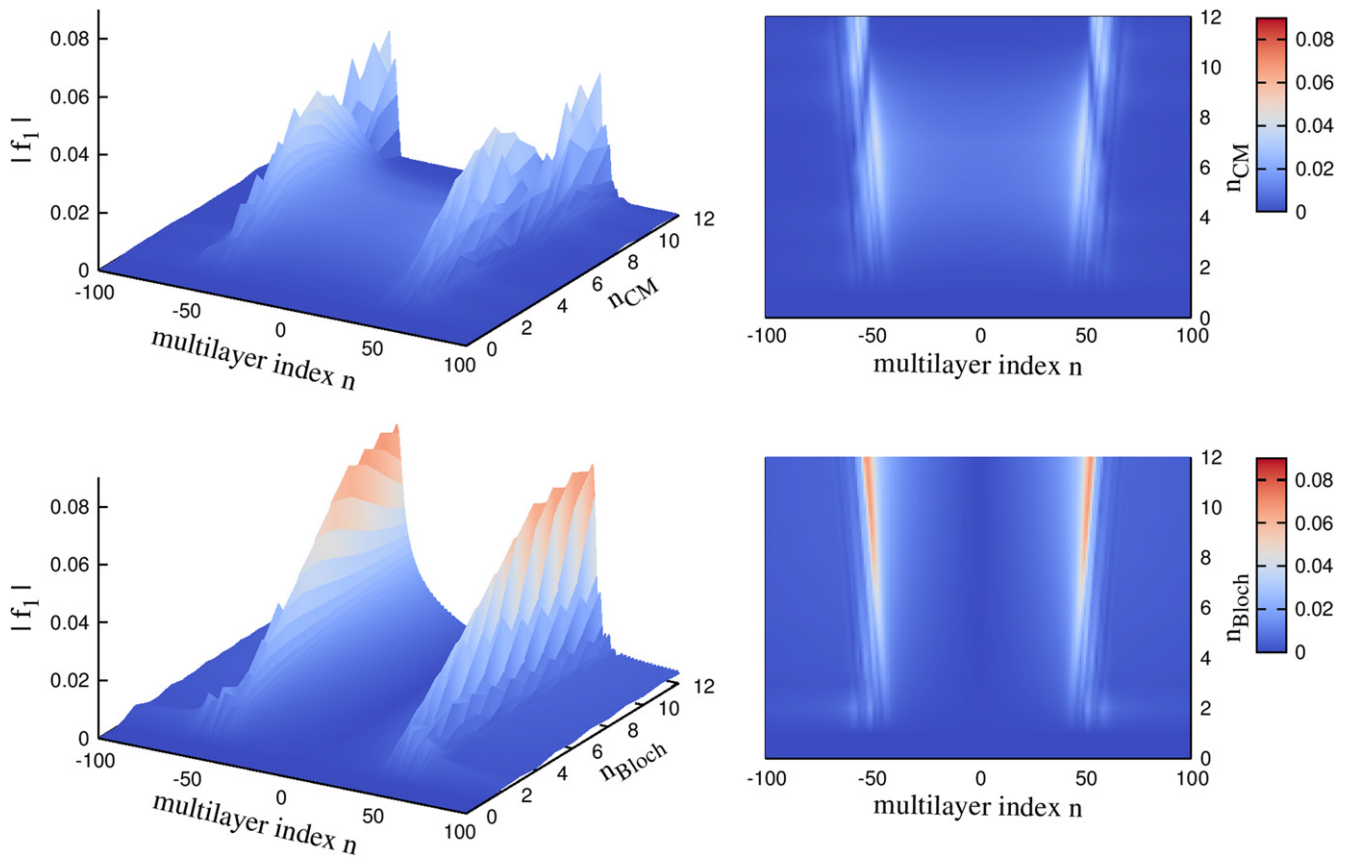


Figure 3. Magnitude of the equal-spin spin-triplet pairing correlations \mathbf{f}_1 for heterostructures containing conical magnetic layers n_{CM} (upper panels), and Bloch domain walls n_{Bloch} (lower panels), respectively. Note that the \mathbf{f}_1 contribution from heterostructures containing Néel domain walls is zero for the chosen geometry (as discussed in the text). The left and right panels both show the full data sets and the right panels show a top view of the data.

magnetic layers of different opening and turning angles leading to different symmetries have been investigated [16, 30] and could be explained with the properties of the \mathbf{f} -vector introduced in (6). The fundamental pairing correlations evaluated according to (6) are shown in figures 2 and 3 for heterostructures containing conical magnetic layers n_{CM} , Bloch domain walls n_{Bloch} , and Néel domain walls $n_{Néel}$, respectively. In particular, the middle panels of figure 2 show the magnitude of the unequal-spin spin-triplet pairing correlations \mathbf{f}_0 for increasing thickness of the Bloch domain wall n_{Bloch} in comparison to conical magnetic layers n_{CM} (upper panels) and Néel domain wall $n_{Néel}$ (lower panels), respectively. The full data sets of the left panels are shown as top views in the respective right panels.

Looking at the oscillations within the FM middle region of the heterostructure, one notices strong oscillations of the unequal-spin spin-triplet pairing correlations \mathbf{f}_0 . This is very similar to heterostructures containing conical magnetic layers (shown in the upper panels). These are essentially the FFLO oscillations discussed above. The magnitude is almost equally strong for thin Bloch domain walls, but decays to smaller values for increasing Bloch domain wall thickness compared to the conical magnetic layers. However, within the interface region the magnitude of \mathbf{f}_0 is increasing linearly with Bloch domain wall thickness and clearly surpasses the strength in

case of the conical magnetic layers. Looking now at figure 3 showing the respective results for the magnitude of the equal-spin spin-triplet pairing correlations \mathbf{f}_1 for heterostructures containing conical magnetic layers n_{CM} (upper panels) and Bloch domain walls n_{Bloch} (lower panels) one immediately notices larger differences. The magnitude of \mathbf{f}_1 rises linearly and is similarly strong for smaller values of Bloch domain wall thickness n_{Bloch} compared to the same thickness of conical magnetic layers n_{CM} . In contrary to the conical magnetic layers, for which \mathbf{f}_1 starts to oscillate and decay with a further increase of layer thickness again, the equal-spin spin-triplet pairing correlations \mathbf{f}_1 for thicker Bloch domain walls increase further and reach saturation for the maximum thickness considered here. Moreover, the overall magnitude of \mathbf{f}_1 for heterostructures containing Bloch domain walls clearly exceeds those for heterostructures containing conical magnetic layers. Finally, a measure for the induced spin magnetic moment provided by the quantity $\mathbf{f} \times \mathbf{f}^*$ of (10) and (11) is shown in figure 4, where again the contributions from heterostructures containing conical magnetic layers n_{CM} , and Bloch n_{Bloch} and Néel $n_{Néel}$ domain walls are shown in the upper, middle, and lower panels, respectively. One immediately notices that spin magnetisation only occurs in the respective interface regions and that no magnetisation leaks into the SC regions of the heterostructures. The overall rise in

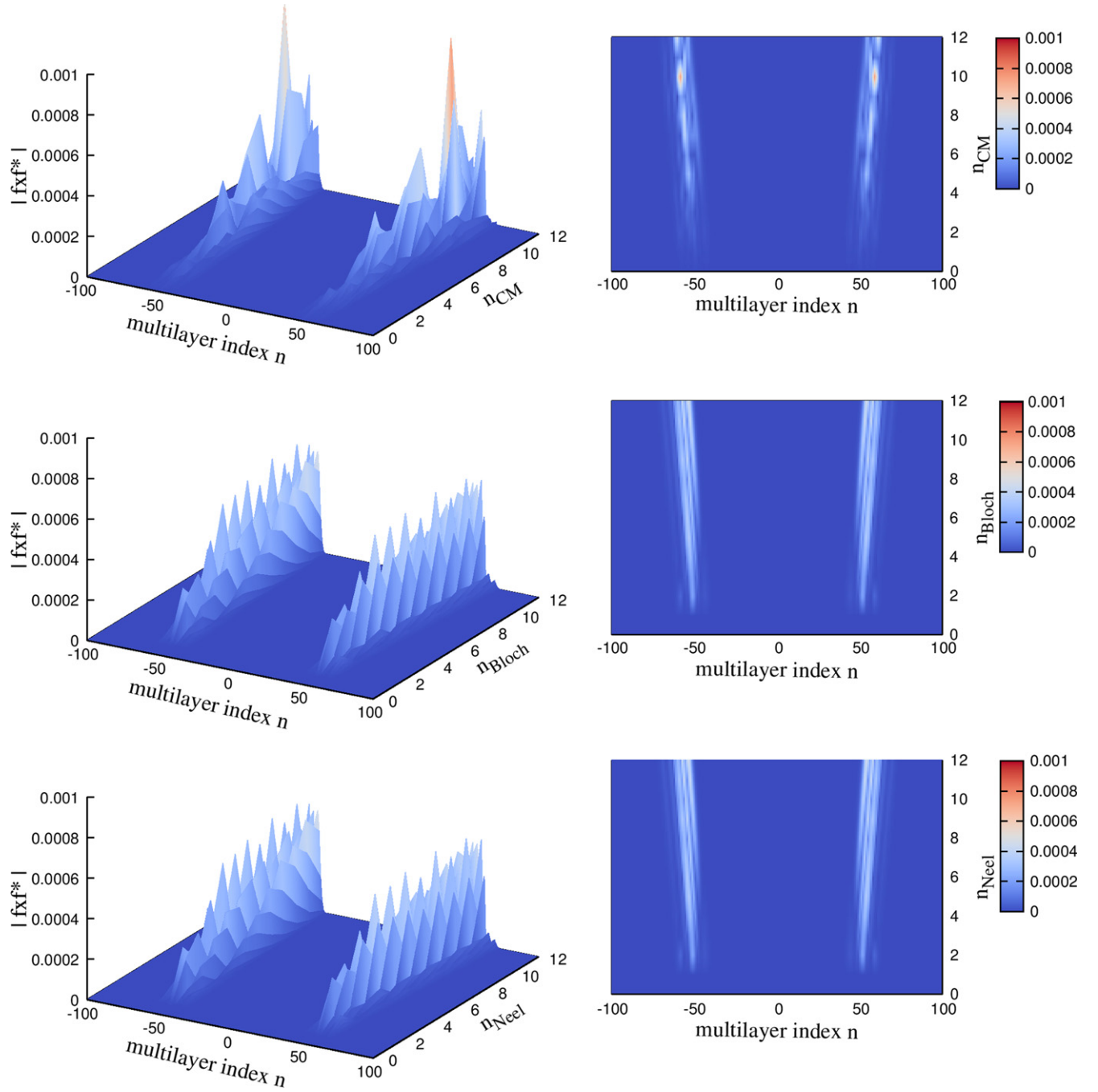


Figure 4. Magnitude of $\mathbf{f} \times \mathbf{f}^*$ for heterostructures containing conical magnetic layers n_{CM} (upper panels), Bloch domain walls n_{Bloch} (middle panels), and Néel domain walls $n_{\text{Néel}}$ (lower panels), respectively. The left and right panels both show the full data sets and the right panels show a top view of the data.

spin magnetisation is stronger for the Bloch domain walls and saturates earlier than in the conical magnetic layers. The latter also show stronger oscillations depending on the thickness n_{CM} compared to the Bloch domain wall thickness n_{Bloch} .

Summarising this we find a similar influence on \mathbf{f}_0 for heterostructures containing conical magnetic layers and Bloch domain walls within the FM middle layer, and a stronger influence within the Bloch domain walls for increasing thickness n_{Bloch} . The magnitude of \mathbf{f}_1 for heterostructures containing Bloch domain walls n_{Bloch} clearly exceeds those

for conical magnetic layers and saturates for the maximum thickness of n_{Bloch} considered here. The measure of induced spin magnetisation provided by $\mathbf{f} \times \mathbf{f}^*$ rises faster and saturates earlier in heterostructures containing Bloch domain walls compared to conical magnetic layers.

3.2. Heterostructure including Néel domain walls

Now we focus on results obtained for heterostructures containing Néel domain walls of increasing thickness $n_{\text{Néel}}$ to

either side of the FM middle layer. They are oriented such that magnetic moments of the Néel domain wall align parallel to the FM middle layers at the interface (figure 1(d)) and are oriented in the yz plane.

Starting the discussion again with the unequal-spin spin-triplet pairing correlations \mathbf{f}_0 shown for Néel domain walls of varying thickness $n_{\text{Néel}}$ in the lower panels of figure 2 one notices that they are nearly indistinguishable to the respective contributions from the Bloch domain walls shown in the middle panels of figure 2. It seems that the orientation of the noncollinear magnetic moments with respect to the interface plane does not influence the induced unequal-spin spin-triplet pairing correlations.

This changes drastically when looking at the equal-spin spin-triplet pairing correlations where we find no contribution stemming from heterostructures containing Néel domain walls (within the particular setup investigated in the present work). This phenomenon has been discussed recently by Alidoust *et al* [14] based on the properties of the triplet anomalous Green's function \mathbf{f} used in their approach. It turns out that for Néel domain walls to successively induce equal-spin spin-triplet pairing correlations \mathbf{f}_1 the respective non-collinear magnetic structure has to occur in the plane parallel to the interface. In the present work the noncollinearity of the Néel domain wall is oriented perpendicular to the interface plane and hence does not contribute towards equal-spin spin-triplet pairing correlations.

Focusing now at the properties of $\mathbf{f} \times \mathbf{f}^*$ shown in figure 4, one notices again that the contributions from heterostructures containing Bloch n_{Bloch} (middle panels) and Néel $n_{\text{Néel}}$ domain walls (lower panels) are again indistinguishable. The spin magnetisation is only present in the interface regions and does not leak into the SC regions of the heterostructures. Again, the overall rise in spin magnetisation is stronger for the Néel domain walls and saturates earlier than in the conical magnetic layers (upper panels). The latter also show stronger oscillations depending on the thickness n_{CM} compared to the Néel domain wall thickness $n_{\text{Néel}}$.

In summary, for the heterostructures containing Néel domain walls we find indistinguishable results for the unequal-spin spin-triplet pairing correlations \mathbf{f}_0 and the measure of the spin magnetisation $\mathbf{f} \times \mathbf{f}^*$ compared to heterostructures containing Bloch domain walls as discussed in section 3.1. However, for the setup chosen for the Néel domain walls we find no induced equal-spin spin-triplet pairing correlations \mathbf{f}_1 at all.

4. Summary and outlook

Here we presented a detailed analysis of spin-triplet pairing correlations occurring in SC/FM/SC heterostructures incorporating different types of noncollinear interface regions of varying thicknesses. Particular interfaces included conical magnetic layers, and Bloch and Néel domain walls. It has been shown that for the unequal-spin spin-triplet pairing correlations \mathbf{f}_0 both Bloch and Néel domain walls exceed the

efficiency provided by conical magnetic layers at the interface. For the equal-spin spin-triplet pairing correlations \mathbf{f}_1 only the Bloch domain walls show considerable improvement over the conical magnetic layer setup, whereas the specific orientation of the Néel domain wall (noncollinear magnetic moments perpendicular to the interface plane) prevented the occurrence of equal-spin spin-triplet pairing correlations in that case. Different orientations of Néel domain walls with respect to the interface plane deserve further investigations. Finally, the dependence of the spin magnetisation $\mathbf{f} \times \mathbf{f}^*$ on the thickness of both, Bloch and Néel domain walls, appears to be smoother compared to the conical magnetic layer setup, but in all cases this stays restricted to the interface region alone.

Acknowledgments

This work has been financially supported by the EPSRC (EP/I037598/1) and made use of computational resources of the University of Bristol.

References

- [1] Buzdin A I, Bulaevskii L N and Panyukov S V 1982 Critical-current oscillations as a function of the exchange field and thickness of the ferromagnetic metal (F) in an S - F - S Josephson junction *JETP Lett.* **35** 178
- [2] Buzdin A I and Kupriyanov M Yu 1991 Josephson junction with a ferromagnetic layer *JETP Lett.* **53** 321
- [3] Demler E A, Arnold G B and Beasley M R 1997 Superconducting proximity effects in magnetic metals *Phys. Rev. B* **55** 15174
- [4] Fulde P and Ferrell R A 1964 Superconductivity in a strong spin-exchange field *Phys. Rev.* **135** A550
- [5] Larkin A I and Ovchinnikov Y N 1965 Inhomogeneous state of superconductors *Sov. Phys.—JETP* **20** 762
- [6] Bergeret F S, Volkov A F and Efetov K B 2001 Long-range proximity effects in superconductor-ferromagnet structures *Phys. Rev. Lett.* **86** 4096
- [7] Buzdin A I 2005 Proximity effects in superconductor-ferromagnet heterostructures *Rev. Mod. Phys.* **77** 935
- [8] Bergeret F S, Volkov A F and Efetov K B 2005 Odd triplet superconductivity and related phenomena in superconductor-ferromagnet structures *Rev. Mod. Phys.* **77** 1321
- [9] Tanaka Y, Sato M and Nagaosa N 2012 Symmetry and topology in superconductors—odd-frequency pairing and edge states *J. Phys. Soc. Japan* **81** 011013
- [10] Klose C *et al* 2012 Optimization of spin-triplet supercurrent in ferromagnet Josephson junctions *Phys. Rev. Lett.* **108** 127002
- [11] Gingrich E C, Quarterman P, Wang Y, Loloee R, Pratt W P Jr and Birge N O 2012 Spin-triplet supercurrent in Co/Ni multilayer Josephson junctions with perpendicular anisotropy *Phys. Rev. B* **86** 224506
- [12] Volkov A F, Anishchanka A and Efetov K B 2006 Odd triplet superconductivity in a superconductor/ferromagnet system with a spiral magnetic structure *Phys. Rev. B* **73** 104412
- [13] Robinson J W A, Witt J D S and Blamire M G 2010 Controlled injection of spin-triplet supercurrents into a strong ferromagnet *Science* **329** 59

- [14] Alidoust M, Linder J, Rhashedi G, Yokoyama T and Sudbø A 2010 Spin-polarized Josephson current in superconductor/ferromagnet/superconductor junctions with inhomogeneous magnetization *Phys. Rev. B* **81** 014512
- [15] Alidoust M and Linder J 2010 Spin-triplet supercurrent through inhomogeneous ferromagnetic trilayers *Phys. Rev. B* **82** 224504
- [16] Fritsch D and Annett J F 2014 Proximity effect in superconductor/conical magnet/ferromagnet heterostructures *New J. Phys.* **16** 055005
- [17] Božović M and Radović Z 2005 Ferromagnet-superconductor proximity effect: the clean limit *Europhys. Lett.* **70** 513
- [18] Linder J, Yokoyama T, Sudbø A and Eschrig M 2009 Pairing symmetry conversion by spin-active interfaces in magnetic normal-metal–superconductor junctions *Phys. Rev. Lett.* **102** 107008
- [19] Linder J, Sudbø A, Yokoyama T, Grein R and Eschrig M 2010 Signature of odd-frequency pairing correlations induced by a magnetic interface *Phys. Rev. B* **81** 214504
- [20] Terrade D, Gentile P, Cuoco M and Manske D 2013 Proximity effects in a spin-triplet superconductor-ferromagnet heterostructure with a spin-active interface *Phys. Rev. B* **88** 054516
- [21] Bergeret F S and Tokatly I V 2013 Singlet-triplet conversion and the long-range proximity effect in superconductor-ferromagnet structures with generic spin dependent fields *Phys. Rev. Lett.* **110** 117003
- [22] Fominov Y V, Volkov A F and Efetov K B 2007 Josephson effect due to the long-range odd-frequency triplet superconductivity in SFS junctions with Néel domain walls *Phys. Rev. B* **75** 104509
- [23] Lv B 2011 Spin triplet Andreev reflection induced by interface spin-orbit coupling in half-metal/superconductor junctions *Eur. Phys. J. B* **83** 493
- [24] Yang Z H, Wang J and Chan K S 2009 Proximity effect in a superconductor/two-dimensional electron gas junction with Rashba spin-orbit coupling *Supercond. Sci. Technol.* **22** 055012
- [25] Annett J F 2004 *Superconductivity, Superfluids and Condensates* (Oxford: Oxford University Press)
- [26] Ketterson J B and Song S N 1999 *Superconductivity* (Cambridge: Cambridge University Press)
- [27] Šipr O and Györfy B L 1995 Oscillatory magnetic coupling between metallic multilayers across superconducting spacers *J. Phys.: Condens. Matter* **7** 5239
- [28] Covaci L and Marsiglio F 2006 Proximity effect and Josephson current in clean strong/weak/strong superconducting trilayers *Phys. Rev. B* **73** 014503
- [29] Fritsch D and Annett J F 2014 Proximity effect in superconductor/conical magnet heterostructures *J. Phys.: Condens. Matter* **26** 274212
- [30] Fritsch D and Annett J F 2015 Spin-flipping with Holmium: case study of proximity effect in superconductor/ferromagnet/superconductor heterostructures *Phil. Mag.* **95** 441
- [31] Balian R and Werthamer N R 1963 Superconductivity with pairs in a relative p wave *Phys. Rev.* **131** 1553
- [32] Sigrist M and Ueda K 1991 Phenomenological theory of unconventional superconductivity *Rev. Mod. Phys.* **63** 239
- [33] Halterman K, Barsic P H and Valls O T 2007 Odd triplet pairing in clean superconductor/ferromagnet heterostructures *Phys. Rev. Lett.* **99** 127002
- [34] Kawabata S, Asano Y, Tanaka Y and Golubov A A 2013 Robustness of spin-triplet pairing and singlet-triplet pairing crossover in superconductor/ferromagnet hybrids *J. Phys. Soc. Japan* **82** 124702